Published in final edited form as:
Lasers Surg Med. 2009 October ; 41(8): 585–594. doi:10.1002/lsm.20839.

Pulsed Dye Laser Induced Inflammatory Response and Extracellular Matrix Turnover in Rat Vocal Folds and Vocal Fold Fibroblasts

Ya Lin, B.S., **Masaru Yamashita, M.D., Ph.D.**, **Jingxian Zhang, Ph.D.**, **Changying Ling, Ph.D.**, and **Nathan V. Welham, Ph.D.**
Division of Otolaryngology, Department of Surgery University of Wisconsin School of Medicine and Public Health Madison, WI, USA

Abstract

Background and Objectives—Disruption of the vocal fold extracellular matrix (ECM) can induce a profound and refractory dysphonia. Pulsed dye laser (PDL) irradiation has shown early promise as a treatment modality for disordered ECM in patients with chronic vocal fold scar; however, there are limited data addressing the mechanism by which this laser energy might induce cellular and extracellular changes in vocal fold tissues. In this study, we examined the inflammatory and ECM modulating effects of PDL irradiation on normal vocal fold tissues and cultured vocal fold fibroblasts.

Study Design/Materials and Methods—We evaluated the effects of 585 nm PDL irradiation on inflammatory cytokine and collagen/collagenase gene transcription in normal rat vocal folds *in vivo* (3–168 h following delivery of ~39.46 J/cm^2 fluence) and vocal fold fibroblasts *in vitro* (3–72 h following delivery of 4.82 or 9.64 J/cm^2 fluence). We also examined morphological vocal fold tissue changes 3 h, 1 week and 1 month post-irradiation.

Results—PDL irradiation altered inflammatory cytokine and procollagen/collagenase expression at the transcript level, both *in vitro* and *in vivo*. Additionally, PDL irradiation induced an inflammatory repair process *in vivo* that was completed by 1 month with preservation of normal tissue morphology.

Conclusions—PDL irradiation can modulate ECM turnover in phenotypically normal vocal folds. Additional work is required to determine if these findings extend to disordered ECM, such as is seen in vocal fold scar.

Keywords

Collagen; Collagenase; Cytokine; Larynx; Photobiology; Tissue remodeling

Introduction

The vocal fold contains a unique tri-layered structure that underpins its biomechanical capacity for phonation. These layers consist of a squamous cell epithelium, a lamina propria (LP) which is abundant in extracellular matrix (ECM), and the thyroarytenoid (TA) muscle. The LP ECM is especially critical to vocal fold tissue viscoelasticity and has a tightly regulated matrix architecture that helps facilitate self-sustained tissue oscillation for phonation (1,2). The primary cell population in the native LP, responsible for ECM turnover

Corresponding Author: Nathan V. Welham, Ph.D. K4/723 CSC, 600 Highland Avenue, Madison, WI 53792, USA. Telephone: +1-608-263-0121; Facsimile: +1-608-252-0939 welham@surgery.wisc.edu.

and maintenance, is the vocal fold fibroblast (VFF) (3). The key components of the ECM believed to be responsible for its structural integrity and favorable viscoelasticity are the fibrous proteins collagen (predominantly types I and III) and elastin, glycoprotein fibronectin, proteogylcans decorin, fibromodulin and versican, and the glycosaminoglycans hyaluronic acid, condroitin sulfate, dermatan sulfate, keratan sulfate and heparan sulfate (1,2,4). Disruption of the vocal fold ECM, particularly due to inflammatory and fibrotic processes, can result in altered tissue viscoelasticity, oscillatory function and voice. Even certain therapeutic interventions to treat or remove diseased tissue can result in residual scarring and poor voice outcomes (5,6). As a result, minimally invasive treatments that result in maximum preservation of ECM structure and function are highly desirable in the treatment of vocal fold pathologies.

The 585 nm pulsed dye laser (PDL) is a non-destructive photoangiolytic laser with clinical precedent in dermatologic aplications (7–9) and documented early promise in the treatment of a range of vocal fold diseases (10–13). Originally developed for the treatment of vascular skin lesions (14), the PDL is commonly used for the treatment of vascular and epithelial lesions in the vocal fold. Its application to vascular lesions is based on the affinity of the PDL wavelength (585 nm) to the upper absorbance peak of oxyhemoglobin (577 nm), allowing uniform vessel penetration and energy delivery to intraluminal blood (10,15). Its application to epithelial lesions is based on the observation that the delivery of PDL energy can result in cleavage of the epithelial cell layer from the underlying superficial LP, hypothesized as due to the denaturation of basement membrane linking proteins (16). In addition to these two therapeutic indications, recent clinical evidence suggests that the PDL may be useful in the treatment of disordered ECM in patients with chronic vocal fold scar (5), although the mechanism by which PDL irradiation might improve ECM structure and function in this population is unknown.

Evidence from the dermal literature suggests that PDL irradiation modulates cell proliferation, inflammatory cytokine and collagen/collagenase expression in both dermis and cultured dermal fibroblasts. Low-dose PDL irradiation has been shown to upregulate the transforming growth factor-β1 (TGFB1) pathway and induce collagen I and III production in photodamaged human skin (17,18) and cultured human dermal fibroblasts (19). In contrast, studies conducted with cultured human keloid fibroblasts indicate that PDL irradiation suppresses cell proliferation and downregulates TGFB1 in this population via the mitogen-activated protein kinase pathway (20,21). Taken together, these data suggest that PDL irradiation induces a differential response according to cell/tissue phenotype.

Previous work focused on the biological mechanism of PDL induced tissue change in the vocal fold has been limited to histological comparison of biopsies from PDL-treated and control human tissues (16). No previous study has investigated the transcriptional and/or translational response of VFFs (either *in vitro* or *in vivo*) to PDL irradiation, and no work has considered a potential mechanism for ECM alteration in the vocal fold. In this study, we subjected cultured rat VFFs and rat vocal folds to PDL irradiation and examined transcriptional changes in the procollagen (COL) genes COL1A1 and COL3A1, the matrix metalloproteinase (MMP) genes MMP8 and MMP13 (considered the primary collagenase genes in rodents), and the inflammatory cytokine genes interleukin-1β (IL1B), interleukin-6 (IL6), TGFB1 and cyclooxygenase-2 (COX2). We also examined morphological vocal fold tissue changes. Our findings indicate that PDL irradiation induces both an inflammatory and ECM modulation response at the transcript level, in addition to an inflammatory repair process that is completed by 1 month with preservation of normal tissue morphology.

Materials and Methods

This study involved PDL irradiation of prolyl 4-hydroxylase β+ rat VFFs *in vitro* (Fig. 1A) and rat membranous vocal folds *in vivo* (Fig. 2A–C). All animal procedures were performed in accordance with the PHS Policy on Humane Care and Use of Laboratory Animals, and the Animal Welfare Act (7 U.S.C et seq.); the animal use protocol was approved by the Institutional Animal Care and Use Committee (IACUC) of the University of Wisconsin-Madison.

Laser

A 585 nm wavelength flashlamp-excited PDL (PhotoGenica SV, Cynosure, Westford, MA, USA) was used in this study. This instrument delivers a 585 nm coherent monochromatic beam with a perfect plane wavefront and Gaussian transverse irradiance profile. The energy delivery range of this laser is 0.5–2.0 J per 450 μs pulse. An energy setting of 0.5 J was used for the *in vivo* experiment; 0.8 J was used for the *in vitro* experiment. All laser energy was delivered via a 600 μm fiber optic cable. Instrument calibration was performed prior to each experimental session.

Initial pilot experimentation was performed using laser alignment paper (Zap-It, Salisbury, NH, USA) to evaluate variation in spot diameter, beam shape and energy distribution as a function of laser energy and laser-target distance (Fig. 1B). Simulating the *in vitro* condition, we found that 0.8 J laser energy delivered from a 22 mm distance resulted in a 6.51 mm spot diameter with uniform energy distribution. This spot diameter closely resembled the 6.5 mm well diameter of the culture plate used in the *in vitro* experiment and allowed the delivery of 2.41 J/cm^2 fluence per pulse. Simulating the *in vivo* condition, we found that 0.5 J laser energy delivered from a 1 mm distance resulted in a 2.2 mm spot diameter with non-uniform energy distribution. This spot diameter allowed irradiation of the entire membranous rat vocal fold with 13.15 J/cm^2 fluence per pulse.

VFF culture

VFF lines, established from normal rat vocal fold explants, were cultured in Dulbecco's modified Eagle medium (DMEM) supplemented with 10% heat-inactivated fetal bovine serum (FBS), 10,000 IU penicillin G potassium, 10 mg/mL streptomycin sulfate, and 25 μg/mL amphotericin B. All cell culture reagents and antibiotics were obtained from Invitrogen (Carlsbad, CA, USA). Fibroblasts were incubated at 37° C in a 5% (v/v) CO_2 humidified atmosphere, and media were changed at 3-day intervals. Fibroblasts from passage 2 were used for the *in vitro* experiment.

PDL irradiation of cultured VFFs

Forty-eight hours prior to laser irradiation, cultured cells were trypsinized, counted using a standard hemocytometer, and plated at a density of 10^3 cells in 0.15 mL medium per well. Cells were plated in every fourth well of a 96-well cultured plate, with no cells in adjacent wells. This plating arrangement was employed to eliminate the possibility of unintended cross-well delivery of laser irradiation. Cells were incubated for 24 h to reach subconfluency and then growth-arrested in serum-free medium for 24 h to reduce the influence of FBS mediated gene expression on experimental results. At the time of laser irradiation, the plate cover was removed, culture media were aspirated, and the cells in each well were treated under one of three conditions: no laser delivery (control), 4.82 J/cm^2 fluence (2 pulses, 0.8 J energy, 22 mm distance, 6.51 mm spot diameter), and 9.64 J/cm^2 fluence (4 pulses, 0.8 J energy, 22 mm distance, 6.51 mm spot diameter). The laser fluence selected for the *in vitro* experiment was based on existing literature addressing PDL irradiation of cultured fibroblasts (19,22). Immediately following irradiation, 0.15 mL of serum free medium was

replaced in each well and cells were incubated for an additional 3, 24, or 72 h before trypsinization and harvest. The entire *in vitro* experiment was replicated four times.

Rat vocal fold PDL irradiation and tissue preparation

Thirty-two 4–6 month old male Sprague Dawley rats (Harlan, Indianapolis, IN, USA) were used for the *in vivo* experiment. Twenty-six rats underwent bilateral vocal fold PDL irradiation and 6 rats were retained as controls. Rats were anesthetized with an intraperitoneal (IP) injection cocktail of ketamine hydrochloride (90 mg/kg) and xylazine hydrochloride (9 mg/kg), followed by IP delivery of atropine sulfate (0.05 mg/kg) to reduce the secretion of saliva and sputum in the laryngeal lumen. Laryngeal visualization was performed as described by Tateya et al. (23). An angled stainless-steel rigid catheter was fabricated to allow passage and directional control of the PDL fiber optic cable under endoscopic guidance (Fig. 2A). The catheter was positioned with the fiber tip in contact with the vocal fold, and then retracted 1 mm prior to tissue irradiation (Fig. 2B–C). Fiber-to-tissue distance was maintained as close to 1 mm as possible throughout the procedure. Each vocal fold was treated with ~39.46 J/cm^2 fluence (3 pulses, 0.5 J energy, ~1 mm distance, ~2.2 mm spot diameter). The laser fluence selected for the *in vivo* experiment was based on published clinical dosing recommendations for human vocal fold tissue (10–13).

Twenty-four larynges intended for real-time RT-PCR analysis were harvested *en bloc* at five time points following PDL irradiation (0 h [control], 3 h, 10 h, 24 h, 72 h, 168 h; 4 larynges per time point). Specimens were embedded in OCT compound (Sakura Finetek Tokyo, Japan), snap frozen using acetone and dry ice, and stored at −80° C. Next, 60 μm whole mount coronal cryosections were prepared using a cryostat and vocal fold lamina propria and epithelial regions were microdissected under a stereo microscope using 30 G needles. All specimen preparation was performed in a sterile RNAse treated environment.

Eight larynges intended for histological analysis and long-term follow-up were harvested en bloc at four time points following PDL irradiation (0 h [control], 3 h, 1 week, 1 month; 2 larynges per time point). Laryngeal tissue was fixed in 4% paraformaldehyde for 48 h and then paraffin embedded.

Real-time RT-PCR

Total RNA was extracted from cells and microdissected tissue samples using the RNeasy Micro Kit (Qiagen, Valencia, CA, USA). Proteinase K digestion was performed for 10 min at 55° C to remove extracellular matrix proteins from the tissue samples prior to RNA isolation and DNase I digestion was performed to remove potentially contaminating genomic DNA. RNA integrity was verified spectrophotometrically by OD_{260}/OD_{280} nm absorbance ratios between 1.8 and 2.0. Reverse transcription (RT) was performed using Superscript III reverse transcriptase (Invitrogen) to synthesize first-strand cDNA. Real-time RT-PCR reactions were performed using a LightCycler 2.0 fluorescence temperature cycler (Roche Diagnostics, Indianapolis, IN, USA). The reaction mix consisted of 2 μL template cDNA, 0.75 μM forward and reverse primers, 1.5 mM MgCl2, 2 μL LightCycler-FastStart DNA Master SYBR Green I mixture (Roche), and RNase free H_2O to a final volume of 20 μL. Samples were incubated for initial denaturing at 95° C for 10 min, followed by 45 cycles, each cycle consisting of 95° C for 15 s, 60° C for 5 s and 72° C for 10 s. Cycle-to-cycle fluorescence emission readings were monitored at 72° C at the end of each cycle and analyzed using the LightCycler software (Roche). Melting curves were generated following each run to confirm the amplification of specific transcripts. All reactions were performed in quadruplicate.

Expression of the following inflammatory cytokine and extracellular matrix genes of interest were examined (gene specific oligonucleotide primers are shown in Table 1): IL1B, IL6, TGFB1, COX2, COL1A1, COL3A1, MMP8, MMP13. Relative quantitative analysis was performed using the standard curve method and ratios of target gene concentration to housekeeping gene ACTB were calculated. Pilot comparison of ACTB with other candidate housekeeping genes 18S ribosomal RNA (rRNA) and glyceraldehyde 3-phosphate dehydrogenase (GAPDH) demonstrated that ACTB held the most stable expression profile across control and laser irradiated samples (data not shown). Therefore, ACTB was used as the housekeeping gene in this study.

Histology and immunocytochemistry

Specimens intended for histological analysis were embedded in paraffin as reported above. Five μm whole-mount coronal sections were cut using a microtome and routine H&E staining was performed. Images were acquired and analyzed using routine bright-field microscopy (Nikon E-600 microscope, Melville, NY, USA; Olympus DP71 camera, Center Valley, PA, USA). Images were analyzed by a medical pathologist, veterinary pathologist, and immune response biologist.

VFFs in passage 2 were subjected to immunostaining for the collagen synthesis enzyme (and fibroblast marker) prolyl 4-hydroxylase β, prior to initiation of the *in vitro* experiment (Fig. 1A). The primary antibody used was mouse anti-rat prolyl 4-hydroxylase β (AF5110-1, 1:200; Acris Antibodies, Hiddenhausen, Germany); the secondary antibody used was Alexa Fluor 488 goat anti-mouse (A11001, 1:200; Invitrogen/Molecular Probes, Eugene, OR, USA). Nuclear staining was performed using Hoechst 33342 (H3570, 0.4 μg/mL; Invitrogen).

Statistical analysis

In vivo real-time RT-PCR data were analyzed using a series of one-way repeated measures analyses of variance (ANOVAs), with time point as a fixed effect. *In vitro* real-time RT-PCR data were analyzed using a series of two-way repeated measures ANOVAs, with time point and laser dose as fixed effects. In each case, a separate ANOVA was performed for each mRNA transcript of interest.

Logarithmic (base e) transformation of the expression ratio of each mRNA transcript relative to the housekeeping gene ACTB was performed a priori in order to better meet the equal variance assumptions of ANOVA. If the omnibus F-test revealed significant differences, pairwise comparisons between the control condition and each experimental condition (time point and/or laser dose) were examined using Fisher's protected least significant difference procedure. An α-level of 0.01 was employed for all statistical testing. All *p*-values were two sided. All computations were performed using SAS version 9.3 for Windows (SAS Institute, Cary, NC, USA).

Results

PDL irradiation alters transcription of ECM and inflammatory cytokine genes in vitro

We treated prolyl 4-hydroxylase β+ rat VFFs (Fig. 1A) with either 4.82 or 9.64 J/cm^2 PDL irradiation. Pilot experimentation confirmed the uniform delivery of laser energy across each culture well surface with no cross-irradiation of adjacent wells (Fig. 1B–D). Fig. 1E summarizes our real time RT-PCR findings for the procollagen genes COL1A1 and COL3A1, the matrix metalloproteinase gene MMP13, and the inflammatory cytokine genes IL1B, IL6, TGFB1 and COX2.

COL1A1 and COL1A3 expression decreased compared to control at all time points following PDL irradiation. For COL1A1, this downregulation reached significance at both doses at 72 h. No significant main effect was observed for PDL dose. COL3A1 downregulation was significant at all time points and doses, with the exception of 3 h 4.82 J/cm^2. A significant main effect was observed for PDL dose, whereby 9.64 J/cm^2 fluence resulted in a significantly greater downregulation of COL3A1 than 4.82 J/cm^2 fluence. A significant dose-time point interaction effect was also observed for COL3A1.

MMP13 expression peaked at 3 h and then decreased at all subsequent time points. In the 4.82 J/cm^2 fluence condition, the initial significant increase at 3 h was followed by significant downregulation compared to control at both 24 and 72 h. In the 9.64 J/cm^2 fluence condition, the initial significant increase identified at 3 h was sustained until 24 h, before switching to significant downregulation at 72 h. No significant main effect was observed for PDL dose, however a significant dose-time point interaction effect was observed.

We examined MMP8 expression in the *in vitro* experiment to confirm absence of transcription by our fibroblast population (MMP8 is a neutrophil collagenase), and to compare with our *in vivo* data. As expected, we did not detect any MMP8 transcripts in either control or PDL irradiated samples (data not shown).

The inflammatory cytokines examined in the *in vitro* experiment demonstrated two distinct expression profiles. IL1B transcription was significantly downregulated at the majority of time points following PDL irradiation, whereas IL6, TGFB1 and COX2 transcription peaked at the 3 h time point and then decreased to various degrees at subsequent time points. For IL6, significant differences were only identified with 9.64 J/cm^2 fluence. For TGFB1, initial upregulation was only significant for 4.82 J/cm^2 fluence and subsequent downregulation reached significance for both doses at 72 h. COX2 was significantly upregulated for both doses at 3 h and returned to control levels by 24 h. No significant main effect was observed for PDL dose for any inflammatory cytokine; a significant dose-time point interaction effect was observed for IL6.

PDL irradiation alters transcription of ECM and inflammatory cytokine genes in vivo

We treated each rat membranous vocal fold with ~39.46 J/cm^2 PDL irradiation, delivered as three 0.5 J pulses at ~1 mm fiber-to-tissue distance (Fig. 2A–C). Fig. 2D–E summarizes our real time RT-PCR findings for the procollagen genes COL1A1 and COL3A1, the matrix metalloproteinase genes MMP8 and MMP13, and the inflammatory cytokine genes IL1B, IL6, TGFB1 and COX2.

COL1A1 and COL1A3 demonstrated similar mRNA expression profiles *in vivo*. For both genes, an initial significant downregulation at 3 h was sustained until 10 h, and followed by significant upregulation at 72 and 168 h. MMP13 demonstrated significant upregulation and peak expression at 3 h, which gradually attenuated over subsequent time points. MMP8 transcripts were not detectable in control tissues and were identified in PDL-treated samples at 10 and 24 h only.

The inflammatory cytokines examined in the *in vivo* experiment demonstrated two distinct expression profiles. TGFB1 demonstrated a trend of gradually increasing expression over time but did not reach significance compared to control, whereas IL1B, IL6 and COX2 expression peaked at 3 h and decreased towards control levels at subsequent time points. For IL1B, initial upregulation was significant at both 3 and 10 h. For IL6, significant differences were identified at 3, 10 and 24 h. COX2 was significantly upregulated at 3 h only.

PDL irradiation induces transient vocal fold tissue inflammation/repair processes in vivo

Rat vocal folds were harvested 3 h, 1 week and 1 month following delivery of ~39.46 J/cm^2 laser fluence. Morphological changes associated with vocal fold PDL irradiation were examined in hematoxylin-eosin (H&E) stained coronal sections. Fig. 3A–H contains representative H&E stained sections for PDL-treated and control samples at each time point.

In naïve rat larynges, the membranous vocal folds were comprised of squamous cell epithelium, LP, and TA muscle (Fig. 3A–B). Three h following PDL irradiation, tissue was characterized by subepithelial edema (Fig. 3C) and red blood cell infiltration in both the subepithelial region (Fig. 3C) and at the deep LP (DLP)-TA muscle junction (Fig. 3D). At 1 week, the epithelium appeared flattened and the LP was marked by increased cellular infiltration, hemosiderins (Fig. 3E), and thrombosed blood vessels surrounded by neutrophils (Fig. 3F). At 1 month, all morphological features of interest appeared comparable to control (Fig 3. G–H).

Discussion

PDL irradiation has demonstrated early promise as a treatment modality for a number of vocal fold diseases, including disordered ECM in patients with chronic vocal fold scar (5); however, there are limited data addressing the mechanism by which this laser energy might induce cellular and extracellular changes in vocal fold tissues. This study represents an experimental assessment of the biological effects of PDL irradiation on vocal fold tissues and cultured vocal fold fibroblasts. Our results indicate that PDL irradiation alters inflammatory cytokine and procollagen/collagenase expression at the transcript level, both *in vitro* and *in vivo*. Additionally, PDL irradiation appears to induce transient morphological changes in vocal fold tissues that resolve by 1 month post-intervention.

We observed a robust inflammatory response to PDL irradiation in both *in vitro* and *in vivo* experiments, characterized by upregulation of inflammatory cytokines, subepithelial edema, blood vessel rupture and cellular infiltration. IL6 and COX2 demonstrated an immediate spike in transcription at 3 h under *in vitro* and *in vivo* conditions, followed by a decrease over time. In contrast, IL1B and TGFB1 demonstrated opposite transcription patterns under *in vitro* and *in vivo* conditions: IL1B was consistently downregulated following irradiation in the *in vitro* experiment but was initially upregulated in the *in vivo* experiment; TGFB1 transcription transitioned from initial upregulation to subsequent downregulation in the *in vitro* experiment but showed no significant difference from control in the *in vivo* experiment. Elevated cytokine signaling is typical following any form of cell or tissue stress (24), and the discrepancies in expression pattern observed for IL1B and TGFB1 *in vitro* and *in vivo* most likely reflect key differences between these experimental systems. Although the isolated response of vocal fold fibroblasts can be well characterized under *in vitro* conditions, these cells are not in their native ECM environment, have no vascular system, and are not subject to interaction with other resident and migrating cell populations, such as the neutrophils observed in the *in vivo* experiment. Leukocytes are known to produce IL1B in the context of a systemic inflammatory response (25), which may explain upregulation of this cytokine in the *in vivo* experiment only.

Collagens I and III are the primary collagen subtypes in human and rat vocal fold LP, where they provide a structural framework and modulate biomechanical stress in the native ECM, and demonstrate elevated abundance and disorganization in the scarred vocal fold ECM (23,26–28). MMPs play a central role in ECM degradation and are therefore essential to matrix turnover and tissue remodeling (29,30). MMP8 and MMP13 have long been considered the primary collagen degrading enzymes in rodents (31), although a potential rodent ortholog to human MMP1 has been reported (32). We observed oppositional

transcription patterns for the procollagen and MMP genes of interest in this study. In our *in vitro* experiment, PDL irradiation induced progressive COL1A1 and COL3A1 downregulation alongside initial upregulation and later downregulation of MMP13. As expected, neutrophil specific MMP8 was not detected. In our *in vivo* experiment, COL1A1 and COL3A1 were initially downregulated but demonstrated significant upregulation beginning at 72 h post-irradiation; whereas MMP8 and MMP13 were initially upregulated and demonstrated no significant difference compared to control beginning at 72 h. The detection of MMP8 transcription at 10 and 24 h post-irradiation in the *in vivo* experiment is consistent with the identification of neutrophils on histological analysis. The sequential and oppositional regulation of procollagen/MMP transcription observed in this study provides support for PDL induced ECM turnover in normal rat vocal folds. Previous work in the dermal literature has demonstrated that PDL irradiation modulates production of COL1A1 and COL3A1 mRNA and procollagen 1 protein in human photodamaged skin (17,18), and that low dose (670 nm non-pulsed) laser irradiation of cutaneous wounds promotes favorable collagen organization during ECM repair and remodeling (33). While the parallels between our data and these reports are encouraging, it is important to note the clear differences between vocal fold mucosa and skin, normal and pathological tissue, and laser modality and delivery settings across studies.

The vessel rupture and red blood cell infiltration observed following PDL irradiation *in vivo* is consistent with high energy absorption by intraluminal blood, due to the affinity of the 585 nm PDL wavelength to the 577 nm upper absorbance peak of oxyhemoglobin (14). Further, our observation of red blood cell accumulation in the subepithelium and at the DLP-TA muscle junction is consistent with preferential vascularization in these regions (34) and may have influenced our *in vivo* findings. Vessel rupture is considered undesirable when treating vocal fold vascular lesions, and so our induction of this response while delivering a clinically relevant dose may reflect procedural imprecision during PDL irradiation (leading to unintended higher dose delivery), differences between rat and human vocal fold microvasculature, and/or the 450 μs pulse width of the PDL instrument used in this study. This relatively short pulse width has been associated with rapid intravascular heating and elevated risk of vessel rupture in vocal fold microvasculature (11,35), and as a result has spurred the development of instruments with pulse widths up to 1.5 ms (15).

We employed three PDL irradiation doses in the *in vitro* and *in vivo* experiments in this study. The *in vivo* dose of ~39.46 J/cm^2 fluence was selected based on published guidelines for the treatment of pathological human vocal fold tissue (10–13); the *in vitro* doses of 4.82 and 9.64 J/cm^2 fluence were purposefully lower than that applied *in vivo* (as we were treating cell monolayers) and were selected based on previous work addressing PDL irradiation of cultured fibroblasts (19,22). We observed a dose effect for COL3A1 and dose-time point interaction effects for MMP13 and IL6. Our observation of reduced COL3A1 transcription in response to higher dose irradiation corresponds to data reported by Yu et al. (19), who observed significantly greater downregulation of COL1A3 in cultured dermal fibroblasts treated with 4 J/cm^2 compared to 3 J/cm^2 PDL fluence. The significance of irradiation dose to our *in vivo* findings is unknown: While the dose employed in this study is considered appropriate for treating vocal fold epithelial and vascular lesions, the optimal dose for ECM remodeling in the vocal fold has not been evaluated in the literature. Given our observations, future work focused on *in vivo* dose optimization should attempt to balance the nature and extent of ECM modulation against the magnitude of inflammatory response and likelihood of vessel rupture.

In this study, we examined the effect of PDL irradiation on phenotypically normal rat vocal folds and cultured vocal fold fibroblasts. While our data suggest that PDL therapy has the potential to modulate ECM turnover, it is important to note that these findings may not

necessarily correspond to disordered ECM, such as is seen in vocal fold scar. This consideration is particularly important given that cultured keloid fibroblasts show a markedly different response to PDL irradiation (20,21) compared to normal cultured dermal fibroblasts (19). Future work in this area should examine the effects of PDL irradiation on both normal and disordered ECM phenotypes, dose optimization, cell proliferation and apoptosis, and matrix deposition and remodeling over time.

Acknowledgments

This study was supported by grant R01 DC004428 from the National Institute on Deafness and Other Communication Disorders and a Hilldale Undergraduate/Faculty Research Award from the University of Wisconsin-Madison. The authors gratefully acknowledge Seth Dailey, M.D. for consultation regarding clinical use of the PDL and its translation to the animal model employed here; Matyas Sandor, Ph.D., Ruth Sullivan, V.M.D., Ph.D., and David Yang, M.D. for assistance with histologic interpretation; and Alejandro Muñoz del Río, Ph.D. for assistance with statistical analysis.

References

1. Pawlak AS, Hammond T, Hammond E, Gray SD. Immunocytochemical study of proteoglycans in vocal folds. Ann Otol Rhinol Laryngol. 1996; 105:6–11. [PubMed: 8546427]
2. Gray SD, Titze IR, Chan R, Hammond TH. Vocal fold proteoglycans and their influence on biomechanics. Laryngoscope. 1999; 109:845–854. [PubMed: 10369269]
3. Catten M, Gray SD, Hammond TH, Zhou R, Hammond E. Analysis of cellular location and concentration in vocal fold lamina propria. Otolaryngol Head Neck Surg. 1998; 118:663–667. [PubMed: 9591866]
4. Hahn MS, Jao CY, Faquin W, Grande-Allen KJ. Glycosaminoglycan composition of the vocal fold lamina propria in relation to function. Ann Otol Rhinol Laryngol. 2008; 117:371–381. [PubMed: 18564535]
5. Mortensen MM, Woo P, Ivey C, Thompson C, Carroll L, Altman K. The use of the pulse dye laser in the treatment of vocal fold scar: A preliminary study. Laryngoscope. 2008; 118:1884–1888. [PubMed: 18641533]
6. Benninger MS, Alessi D, Archer S, Bastian R, Ford C, Koufman J, Sataloff RT, Spiegel JR, Woo P. Vocal fold scarring: Current concepts and management. Otolaryngol Head Neck Surg. 1996; 115:474–482. [PubMed: 8903451]
7. Wu JJ, Papajohn NG, Murase JE, Verkruysse W, Kelly KM. Generalized chrysiasis improved with pulsed dye laser. Dermatol Surg. 2009; 35:538–542. [PubMed: 19292841]
8. Bowes LE, Alster TS. Treatment of facial scarring and ulceration resulting from acne excoriee with 585-nm pulsed dye laser irradiation and cognitive psychotherapy. Dermatol Surg. 2004; 30:934–938. [PubMed: 15171775]
9. Lack EB, Rachel JD. Resolution of retracted scar after 585-nm pulse dye laser surgery. J Cosmet Laser Ther. 2004; 6:149–151. [PubMed: 15545099]
10. Zeitels SM, Burns JA. Laser applications in laryngology: Past, present, and future. Otolaryngol Clin North Am. 2006; 39:159–172. [PubMed: 16469661]
11. Zeitels SM, Akst LM, Bums JA, Hillman RE, Broadhurst MS, Anderson RR. Pulsed angiolytic laser treatment of ectasias and varices in singers. Ann Otol Rhinol Laryngol. 2006; 115:571–580. [PubMed: 16944655]
12. Franco RA Jr. Zeitels SM, Farinelli WA, Faquin W, Anderson RR. 585-nm pulsed dye laser treatment of glottal dysplasia. Ann Otol Rhinol Laryngol. 2003; 112:751–758. [PubMed: 14535557]
13. Franco RA Jr. Zeitels SM, Farinelli WA, Anderson RR. 585-nm pulsed dye laser treatment of glottal papillomatosis. Ann Otol Rhinol Laryngol. 2002; 111:486–492. [PubMed: 12090703]
14. Anderson RR, Parrish JA. Selective photothermolysis: precise microsurgery by selective absorption of pulsed radiation. Science. 1983; 220:524–527. [PubMed: 6836297]
15. Burns JA, Kobler JB, Heaton JT, Anderson RR, Zeitels SM. Predicting clinical efficacy of photoangiolytic and cutting/ablating lasers using the chick chorioallantoic membrane model:

Implications for endoscopic voice surgery. Laryngoscope. 2008; 118:1109–1124. [PubMed: 18354337]

16. Ayala C, Selig M, Faquin W, Franco RA Jr. Ultrastructural evaluation of 585-nm pulsed-dye laser-treated glottal dysplasia. J Voice. 2007; 21:119–126. [PubMed: 16457987]
17. Orringer JS, Voorhees JJ, Hamilton T, Hammerberg C, Kang S, Johnson TM, Karimipour DJ, Fisher G. Dermal matrix remodeling after nonablative laser therapy. J Am Acad Dermatol. 2005; 53:775–782. [PubMed: 16243125]
18. Orringer JS, Hammerberg C, Hamilton T, Johnson TM, Kang S, Sachs DL, Fisher G, Voorhees JJ. Molecular effects of photodynamic therapy for photoaging. Arch Dermatol. 2008; 144:1296–1302. [PubMed: 18936392]
19. Yu HY, Chen DF, Wang Q, Cheng H. Effects of lower fluence pulsed dye laser irradiation on production of collagen and the mRNA expression of collagen relative gene in cultured fibroblasts in vitro. Chin Med J (Engl). 2006; 119:1543–1547. [PubMed: 16996008]
20. Kuo YR, Wu WS, Wang FS. Flashlamp pulsed-dye laser suppressed TGF-beta1 expression and proliferation in cultured keloid fibroblasts is mediated by MAPK pathway. Lasers Surg Med. 2007; 39:358–364. [PubMed: 17457842]
21. Kuo YR, Wu WS, Jeng SF, Huang HC, Yang KD, Sacks JM, Wang FS. Activation of ERK and p38 kinase mediated keloid fibroblast apoptosis after flashlamp pulsed-dye laser treatment. Lasers Surg Med. 2005; 36:31–37. [PubMed: 15662632]
22. Glassberg E, Lask GP, Tan EM, Uitto J. Cellular effects of the pulsed tunable dye laser at 577 nanometers on human endothelial cells, fibroblasts, and erythrocytes: An in vitro study. Lasers Surg Med. 1988; 8:567–572. [PubMed: 3210881]
23. Tateya T, Tateya I, Sohn JH, Bless DM. Histologic characterization of rat vocal fold scarring. Ann Otol Rhinol Laryngol. 2005; 114:183–191. [PubMed: 15825566]
24. McIntire CR, Yeretssian G, Saleh M. Inflammasomes in infection and inflammation. Apoptosis. 2009; 14:522–535. [PubMed: 19156527]
25. Dinarello CA. Immunological and inflammatory functions of the interleukin-1 family. Annu Rev Immunol. 2009; 27:519–550. [PubMed: 19302047]
26. Hirano S, Minamiguchi S, Yamashita M, Ohno T, Kanemaru SI, Kitamura M. Histologic characterization of human scarred vocal folds. J Voice. 2009; 23:399–407. [PubMed: 18395421]
27. Gray SD, Titze IR, Alipour F, Hammond TH. Biomechanical and histologic observations of vocal fold fibrous proteins. Ann Otol Rhinol Laryngol. 2000; 109:77–85. [PubMed: 10651418]
28. Tateya T, Tateya I, Bless DM. Collagen subtypes in human vocal folds. Ann Otol Rhinol Laryngol. 2006; 115:469–476. [PubMed: 16805380]
29. Birkedal-Hansen H. Proteolytic remodeling of extracellular matrix. Curr Opin Cell Biol. 1995; 7:728–735. [PubMed: 8573349]
30. Birkedal-Hansen H, Moore WG, Bodden MK, Windsor LJ, Birkedal-Hansen B, DeCarlo A, Engler JA. Matrix metalloproteinases: A review. Crit Rev Oral Biol Med. 1993; 4:197–250. [PubMed: 8435466]
31. Jeffrey, JJ. Collagenase 3. In: Barrett, AJ.; Rawlings, ND.; Woessner, JF., editors. Handbook of proteolytic enzymes. Academic Press; London: 1998. p. 1167-1170.
32. Balbin M, Fueyo A, Knauper V, Lopez JM, Alvarez J, Sanchez LM, Quesada V, Bordallo J, Murphy G, Lopez-Otin C. Identification and enzymatic characterization of two diverging murine counterparts of human interstitial collagenase (MMP-1) expressed at sites of embryo implantation. J Biol Chem. 2001; 276:10253–10262. [PubMed: 11113146]
33. Medrado AP, Soares AP, Santos ET, Reis SR, Andrade ZA. Influence of laser photobiomodulation upon connective tissue remodeling during wound healing. J Photochem Photobiol B. 2008; 92:144–152. [PubMed: 18602833]
34. Lyon, MJ.; Barkmeier-Kraemer, JM. Vascular supply of the larynx. In: Sapienza, CM.; Casper, JK., editors. Vocal Rehabilitation in Medical Speech-Language Pathology. Pro-Ed; Austin: 2004. p. 69-108.
35. Broadhurst MS, Akst LM, Burns JA, Kobler JB, Heaton JT, Anderson RR, Zeitels SM. Effects of 532 nm pulsed-KTP laser parameters on vessel ablation in the avian chorioallantoic membrane: Implications for vocal fold mucosa. Laryngoscope. 2007; 117:220–225. [PubMed: 17204988]

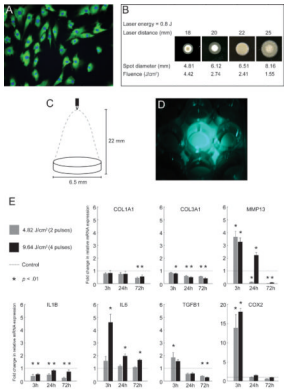

Figure 1.

In vitro experimental procedures and real time RT-PCR analysis showing expression of select ECM and inflammatory cytokine genes in PDL-treated VFFs. A: Representative immunostain of VFFs positive for prolyl 4-hydroxylase β (green). Cell nuclei are stained with Hoechst 33342 (blue). B: Results of pilot experimentation using Zap-It laser alignment paper to evaluate variation in spot diameter, beam shape and energy distribution as a function of laser energy and laser-target distance. Uniform energy distribution within a 6.51 mm spot diameter was obtained with 0.8 J laser energy delivered from a 22 mm distance, and these parameters were selected for subsequent experimentation. C: Schematic illustrating PDL laser delivery for the *in vitro* experiment using the parameters indentified in B. The culture well diameter (6.5 mm) closely matched the laser spot diameter (6.51 mm). D: Photograph illustrating laser energy delivery across each culture well surface with no cross-irradiation of adjacent wells. This image was captured using the 505 nm aiming laser on the PDL instrument. E: Fold change in relative mRNA expression of COL1A1, COL3A1, MMP13, IL1B, IL6, TGFB1 and COX2 in PDL-treated fibroblasts compared to control, 3, 24 and 72 h following delivery of either 4.82 or 9.64 J/cm^2 laser fluence. Data represent four independent experimental replicates. ACTB was employed as a housekeeping gene.

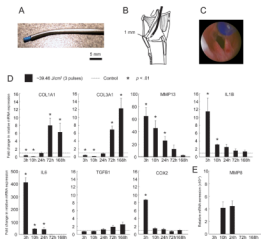

Figure 2.

In vivo experimental procedures and real time RT-PCR analysis showing expression of select ECM and inflammatory cytokine genes in PDL-treated vocal folds. A: Angled stainless-steel rigid catheter allowing passage and directional control of the PDL fiber optic cable under endoscopic guidance. B: Schematic showing the catheter positioned with the fiber tip 1 mm above the membranous vocal fold surface. C: Endoscopic image showing the fiber tip positioned 1 mm above the membranous vocal fold surface prior to tissue irradiation. D: Fold change in relative mRNA expression of COL1A1, COL3A1, MMP13, IL1B, IL6, TGFB1 and COX2 in PDL-treated vocal folds compared to control, 3–168 h following delivery of ~39.46 J/cm^2 laser fluence. E: Relative mRNA expression of MMP8 in PDL-treated vocal folds, 3–168 h following delivery of ~39.46 J/cm^2 laser fluence. MMP8 was not detected in control, 3 h, 72 h and 168 h samples. Data represent four animals per time point. ACTB was employed as a housekeeping gene.

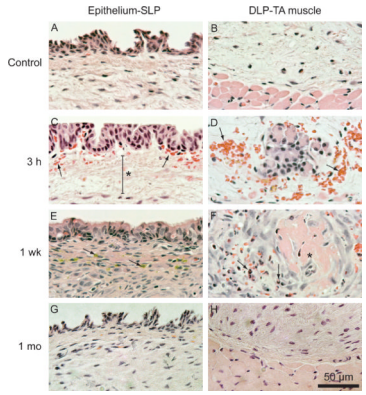

Figure 3.

Representative hematoxylin-eosin stained vocal fold sections of tissue harvested 3 h, 1 week and 1 month following delivery of ~39.46 J/cm^2 laser fluence. A: Control section showing the epithelium and superficial lamina propria (SLP). B: Control section showing the deep lamina propria (DLP) and thyroarytenoid (TA) muscle. C: Subepithelial red blood cell infiltration (arrows) and edema (asterisk) at 3 h. D: Red blood cell infiltration at the DLP-TA muscle junction at 3 h. E: Flattened epithelium, increased cellular infiltration to the lamina propria, and hemosiderin (arrows) at 1 week. F: Thrombosed blood vessel (asterisk) surrounded by neutrophils (arrows) at 1 week. G: Epithelium and SLP comparable to control at 1 month. H: DLP and TA muscle comparable to control at 1 month.

Table 1

Primers sequences used for real-time RT-PCR.

Gene	Primers
ACTB	Fwd: 5'-TGA GCG CAA GTA CTC TGT GTG GAT-3'
	Rvs: 5'-AGA AGC ATT TGC GGT GCA CGA T-3'
IL1B	Fwd: 5'-AGG ATT GCT TCC AAG CCC TTG ACT-3'
	Rvs: 5'-ACA GCT TCT CCA CAG CCA CAA TGA-3'
IL6	Fwd: 5'-CAA GAG ACT TCC AGC CAG TTG C-3'
	Rvs: 5'-TGT TGT GGG TGG TAT CCT CTG TG-3'
TGFB1	Fwd: 5'-TGG CGT TAC CTT GGT AAC C-3'
	Rvs: 5'-GGT GTT GAG CCC TTT CCA G-3'
COX2	Fwd: 5'- TCC AGT ATC AGA ACC GCA TTG CCT-3'
	Rvs: 5'-AGC AAG TCC GTG TTC AAG GAG GAT-3
COL1A1	Fwd: 5'-AGG CAT AAA GGG TCA TCG TGG CTT-3'
	Rvs: 5'-AGT CCA TCT TTG CCA GGA GAA CCA-3'
COL3A1	Fwd: 5'-ATG AGC TTT GTG CAA TGT GGG ACC-3'
	Rvs: 5'-ACT GAC CAA GGT AGT TGC ATC CCA-3'
MMP8	Fwd: 5'-TGG ACA CAC ACT AAC CTG ACC TAC-3'
	Rvs: 5'-TCT CCC TCT AAG GTC TCA GTG AAG-3'
MMP13	Fwd: 5'-AAA GAA CAT GGT GAC TTC TAC C-3'
	Rvs: 5'-ACT GGA TTC CTT GAA CGT C-3'

Note: ACTB, β-actin; TGFB1, transforming growth factor-β1; COX2, cyclooxygenase-2; IL1B, interleukin-1β; IL6, interleukin-6; COL1A1, collagen type 1 α1; COL3A1, collagen type 3 α1; MMP8, matrix metalloproteinase 8; MMP13, matrix metalloproteinase 13. Standard gene symbols were obtained from the HUGO Gene Nomenclature Committee (http://www.genenames.org).